Oil Shale, 2021, Vol. 38, No. 2, pp. 119–136
doi: https://doi.org/10.3176/oil.2021.2.02
ISSN 0208-189X

Study on the permeability of oil shale during in situ pyrolysis

Li Li[a,b], Jian Liu[c,d,e,f,g]*, Yide Geng[g]

[a] School of Geosciences and Info-physics, Central South University, Changsha, Hunan 410012, China
[b] Shanxi Earthquake Agency, Taiyuan, Shanxi 030021, China
[c] College of Earth Science and Engineering, Hebei University of Engineering, Handan, Hebei 056038, China
[d] Department of Geological Engineering, Shanxi Institute of Energy, Jinzhong, Shanxi 030600, China
[e] Collaborative Innovation Center for Comprehensive Development and Utilization of Coal Resources, Hebei Province, Handan, Hebei 056038, China
[f] Key Laboratory of Resource Survey and Research of Hebei Province, Handan, Hebei 056038, China
[g] Key Laboratory of In-situ Property-improving Mining of Ministry of Education, Taiyuan, Shanxi 030024, China

Received 11.06.2020, accepted 16.05.2021, available online 10.06.2021

Abstract. *It is of great significance to quantitatively study the permeability of oil shale and its variation during in situ pyrolysis, which can be used to predict the hydrogeological environment changes induced by the in situ pyrolysis process. Since oil shale permeability during in situ pyrolysis cannot be directly measured in real time, a systematic analysis of pyrolysis kinetics and mechanism, combined with thermogravimetric experiments, allow a constitutive model of the porosity and elastic modulus of oil shale to be deduced. In analyzing the stress and strain mechanism of oil shale under in situ conditions, combined with the quantitative relationship between porosity and permeability, a constitutive permeability model of oil shale during in situ pyrolysis was established. Meanwhile, the predicted variation of oil shale permeability during in situ pyrolysis was compared with experimental results.*

Keywords: *oil shale, in situ pyrolysis, permeability, constitutive model, variation law.*

* Corresponding author: e-mail *5102135@163.com*

1. Introduction

In situ pyrolysis is an emerging oil shale mining method that generates shale oil and related gaseous products by direct injection of heat into the underground oil shale layer [1, 2]. Compared with traditional methods of mining such as well mining and surface dry distillation, the in situ pyrolysis has the advantages of lower-intensity processing, lower cost, higher efficiency, and a smaller physical footprint, which render it a key mining method in the future. However, after in situ pyrolysis oil shale is loose and porous, and its permeability significantly changes, which adversely affects the hydrogeological environment and groundwater flow field in the mining area, inducing even groundwater pollution.

In recent years, scholars have carried out studies on changes in the permeability characteristics of oil shale caused by pyrolysis. For example, Kang [3] measured the porosity of oil shale from the Fushun west open-pit mine at different temperatures and found no significant changes in it at temperatures from normal to 300 °C. Above 300 °C, the porosity remarkably increased with increasing temperature. Kang et al. [4] studied the internal pore characteristics of oil shale under different temperature conditions by using micro-computed tomography (CT) technology, and established that the pores formed during pyrolysis were the controlling factor of oil shale permeability change and that the two factors, porosity and permeability, were highly correlated with each other. Eseme et al. [5] conducted high-temperature triaxial compression experiments on oil shale formed in six different geological periods and observed that the porosity of oil shale was low and that further the porosity of the compressed oil shale decreased; however, it gradually increased with increasing temperature and output of oil and gas products. Tiwari et al. [6] investigated the development and formation of internal pores before and after pyrolysis of the U.S. Green River oil shale and found that a large number of pore structures were formed inside oil shale after pyrolysis and that permeability sharply increased. Zhao [7] used CT methods to measure the porosity of oil shales in the Fushun west open-pit mine and Laohei Mountain in Daqing and noticed it to increase with increasing temperature. The researchers used model fitting to determine the relationship between oil shale porosity and temperature. Jiang [8] measured the porosity of Fuyu oil shale before and after pyrolysis and discovered that it was higher at higher temperatures. At room temperature the porosity was 2.55%, then increased to 10.12% at 300 °C, reaching 19.05% at 500 °C. Qiu [9] found that the porosity and permeability of the oil shale layer significantly increased after pyrolysis, while the enlarged pore cracks resulted in hydraulic connections between the oil shale layer and adjacent aquifers, which might bring pyrolysis pollutants into the aquifers and lead to groundwater pollution. Bai et al. [10] studied the evolution of the pore structure of Huadian oil shale in the temperature range of 100–800 °C. The results showed that this process was significantly influenced

by temperature, while the oil shale porosity and permeability increased with increasing temperature. Burnham [11] investigated changes in the porosity and permeability of Green River oil shale during retorting under confinement, and established a related statistical mathematical model based on the fitting results of a large amount of data. Geng et al. [12–15] observed that under the effects of temperature and pressure, the pore fracture structure of oil shale underwent a fundamental and irreversible change, which rendered it from a low-porosity rock at room temperature to a material with highly developed pore fractures after high-temperature and high-pressure pyrolysis, while its permeability also changed synchronously.

The current research is primarily focused on the comparative study of the porosity and permeability of oil shale before and after pyrolysis. At the same time, studies on changes in oil shale permeability with pyrolysis degree during in situ process have been rarely reported. This may be explained by the fact that it is difficult to observe the oil shale pyrolysis process continuously in real time, which hampers achieving the necessary oil shale permeability during the process on time and studying the induced changes in the hydrogeological environment. In the current research, the qualitative descriptions and quantitative expressions are based on statistics and fitting only. So far, few researchers have established and analyzed quantitative models of oil shale permeability change during the in situ pyrolysis process from a mechanistic perspective.

Before large-scale industrial implementation of in situ pyrolysis technology, it is urgent to establish a mechanism-based quantitative model of oil shale permeability and study the law of related changes during the in situ pyrolysis process. This will be of great significance for the prediction of resulting hydrogeological environmental changes in the mining area. In this paper, oil shale from the Fushun west open-pit mine is used as a research object.

2. Methods

Oil shale is mainly composed of minerals and organic matter. Minerals form its skeleton part, which is often evenly and finely mixed with organic matter. Organic matter fills most of the pores of the mineral skeleton. Kerogen is the main form of organic matter in oil shale, and the essence of oil shale pyrolysis is the pyrolysis of kerogen. Kerogen will pyrolyze, eventually forming products such as shale oil and pyrolysis gas. The pyrolysis process model of Fushun oil shale is described as Equation (1) [16]):

$$\text{Kerogen} \rightarrow \text{Asphalt} \xrightarrow{k} \text{Shale Oil} + \text{Pyrolysis Gas} + \text{Carbon Residue}. \quad (1)$$

With the precipitation of pyrolysis products, oil shale gradually becomes loose and porous, which leads to changes in porosity and permeability.

It is well known that oil shale permeability is closely related to porosity, and the two are usually positively correlated. Under in situ conditions, due to the confining pressure, oil shale undergoes compressive deformation, causing porosity changes, which affects its permeability. The deformation property of oil shale under pressure can be characterized by the elastic modulus. Therefore, to study the law of oil shale permeability change during in situ pyrolysis, it is necessary to establish a quantitative relationship between permeability, porosity and the elastic modulus. This consists in constructing models of oil shale porosity and elastic modulus, on the basis of which a model of oil shale porosity change during the in situ pyrolysis process is proposed. Then, combined with the quantitative relationship between permeability and porosity, a quantitative model of oil shale permeability change during the in situ pyrolysis can eventually be constructed and the variation law of permeability can be studied.

2.1. Model of oil shale porosity during pyrolysis

The above analysis shows that the oil shale porosity changes mainly during the pyrolysis of its organic matter kerogen. Assuming that the pyrolysis products of kerogen generated escape immediately, the variation of oil shale porosity during pyrolysis can be expressed as Equation (2):

$$n' = n_c + \Delta n = n_c + \frac{m \cdot \alpha / \rho_o - m_c \cdot \alpha / \rho_c}{M / \rho_s} \times 100\% = n_c + \frac{p_o \cdot \alpha \cdot \rho_s}{\rho_o} - \frac{p_c \cdot \alpha \cdot \rho_s}{\rho_c}, \quad (2)$$

where n' is the porosity of oil shale during pyrolysis, n_c is the initial porosity of oil shale, Δn is the variation of oil shale porosity during pyrolysis, M is the mass of oil shale, m is the mass of kerogen, m_c is the mass of carbon residue, ρ_s is the density of oil shale, ρ_o is the density of kerogen, ρ_c is the density of carbon residue, α is the pyrolysis ratio of kerogen, p_o is the content of kerogen, and p_c is the content of residual carbon in oil shale.

2.2. Elastic modulus model of oil shale during pyrolysis

Under high temperature conditions, oil parent material will melt from solid to liquid. During this process, the pore pressure in oil shale is mainly exerted by the melted kerogen. According to the principle of effective stress [17] due to which the overburden remains unchanged, the pore pressure gradually decreases and the effective stress increases with the pyrolysis of kerogen, which eventually leads to the compression of oil shale, directly manifested as the change of the elastic modulus. During the pyrolysis process, the decomposition of kerogen will cause a decrease of pore pressure and an increase of effective stress. Eventually, oil shale will be compressed, which directly results in a decrease of the elastic modulus. In addition, the reduction

of the compressive strength of the oil shale skeleton at high temperature will also affect the elastic modulus. In conclusion, the change in the effective stress and the decrease in skeleton strength in the pyrolysis process are the main reasons for the decrease in the elastic modulus of oil shale.

In the case of equal strain, the elastic modulus model of oil shale during pyrolysis can be expressed as follows:

$$\frac{\sigma}{E} = \frac{\sigma_t}{E_t} = \frac{\sigma' + u_t}{E_t}, \tag{3}$$

$$E_t = \frac{E \cdot (\sigma' + u_t)}{\sigma} = \frac{E \cdot [\sigma' + u \cdot (1-\alpha)]}{\sigma}, \tag{4}$$

where E_t, σ_t and u_t are the elastic modulus, compressive strength and pore pressure of oil shale during pyrolysis, respectively; E, σ and u are the elastic modulus, compressive strength and pore pressure of oil shale before pyrolysis, respectively; and σ' is the compressive strength of the oil shale skeleton.

2.3. Pyrolysis rate equation of oil shale

The Coats-Redfern (C-R) method [16, 18–21] was applied to analyze the mass-temperature curve of oil shale obtained in the thermogravimetric experiment.

$$ln\left[\frac{-ln(1-\alpha)}{T^2}\right] = ln\frac{AR}{\beta D} - \frac{D}{RT}, \tag{5}$$

The kinetic equation obeyed by this method is as follows:

where A is the frequency factor, min^{-1}; R is the gas constant, 8.314 J/(mol·K); β is the heating rate, °/min; and D is the activation energy, kJ/mol.

Through the linear fitting of $\ln\left[\frac{-\ln(1-\alpha)}{T^2}\right]$ and $\frac{1}{T}$, A and D can be obtained from the intercept $\ln\left(\frac{AR}{\beta D}\right)$ and the slope $-\frac{D}{R}$ of the fitted line, respectively, and the pyrolysis rate constant k of oil shale at any temperature T can be calculated as follows:

$$k = A \cdot e^{-D/RT}. \tag{6}$$

Then, the pyrolysis rate equation of oil shale at any temperature T can be obtained:

$$\frac{d\alpha}{dt} = k \cdot (1-\alpha). \tag{7}$$

By integrating Equation (7), the pyrolysis rate equation can be written as follows:

$$\alpha = 1 - e^{-kt}. \tag{8}$$

2.4. Model of oil shale permeability during in situ pyrolysis

2.4.1. Model of oil shale porosity during in situ pyrolysis

Under in situ conditions, the porosity of oil shale is related to the elastic modulus. Under the same pressure conditions, the smaller the elastic modulus, the larger the oil shale deformation and the greater the porosity change.

In order to establish a simple yet comprehensive model to reflect the real in situ conditions, the following basic assumptions are made in this study:

1) The compression deformation of oil shale is a linear elastic deformation.
2) The compression deformation of oil shale is manifested as the shrinkage of its internal pores.
3) No new cracks are formed in oil shale during the compression deformation.
4) The horizontal confining pressures are equal:

$$\sigma_2 = \sigma_3 = \frac{\sigma_1 \cdot \mu}{1-\mu}. \tag{9}$$

On the basis of assumption 4), combined with the rock mechanics theory [17], the following relationships are derived:

$$\sigma_m = \frac{\sigma_1 + \sigma_2 + \sigma_3}{3} = \frac{\sigma_1(1+\mu)}{3(1-\mu)}, \tag{10}$$

$$E_k = \frac{E_t}{3(1-2\mu)}, \tag{11}$$

$$\varepsilon_k = \frac{\sigma_m}{E_k} = \frac{\sigma_1(1+\mu)(1-2\mu)}{(1-\mu)E_t}. \tag{12}$$

The model of oil shale porosity under in situ conditions is established as follows:

$$n'' = \frac{V_p - V_t \cdot \varepsilon_k}{V_t(1-\varepsilon_k)} = \frac{n' - \varepsilon_k}{1-\varepsilon_k}, \tag{13}$$

where n'' is the porosity of oil shale during in situ pyrolysis, $n' = \frac{V_p}{V_t}$ is the porosity of oil shale during pyrolysis with no confining pressure, V_p is the pore volume of oil shale during pyrolysis with no confining pressure, V_t is the volume of oil shale during pyrolysis with no confining pressure, ε_k is the volumetric strain of oil shale during pyrolysis under pressure, E_k is the bulk modulus of oil shale during pyrolysis with no pressure, μ is Poisson's ratio of oil shale, and σ_1, σ_2 and σ_3 are the principal stresses.

2.4.2. Quantitative relationship between oil shale porosity and permeability

The constitutive relationship between rock permeability and porosity is complex, and there is currently no corresponding physical constitutive model available. In this study, the quantitative relationship between oil shale porosity and permeability is established by fitting.

2.4.3. Model of oil shale permeability during in situ pyrolysis

The oil shale permeability model during in situ pyrolysis can be obtained by substituting the porosity model by the relationship between porosity and permeability fitting.

3. Results and discussion

3.1. Pyrolysis reaction rate equation of oil shale

Based on thermogravimetric (TG) analysis experiments, TG and differential thermogravimetric (DTG) curves of oil shale pyrolysis in the Fushun west open-pit mine were obtained (Fig. 1). The curves clearly show that the pyrolysis of oil shale mainly occurs in the temperature range of 300–600 °C [3]. At this stage, kerogen is mostly pyrolyzed to give shale oil and gaseous products. The TG curve declines rapidly and sharply, the maximum peak value appears on the DTG curve and the weight loss is large, accounting for approximately 16.21% of the sample mass. However, a previous study [22] found that in the range of 300–500 °C, the variations in the porosity, elastic modulus and compressive strength of the Fushun west open-pit mine oil shale sharply increased, while these variations were slight in the range of 500–600 °C. It was believed that the pyrolysis of oil shale mostly occurred at 300–500 °C, and that of other substances, such as fixed carbon, took place in the range of 500–600 °C. Therefore, in this paper, the pyrolysis temperature range is determined to be 300–500 °C.

Based on the above research methods and thermogravimetric curve data, $\ln\left[\frac{-\ln(1-\alpha)}{T^2}\right]$ and $\frac{1}{T}$ in the pyrolysis stage (300–500 °C) were linearly fitted, the results are shown in Figure 2.

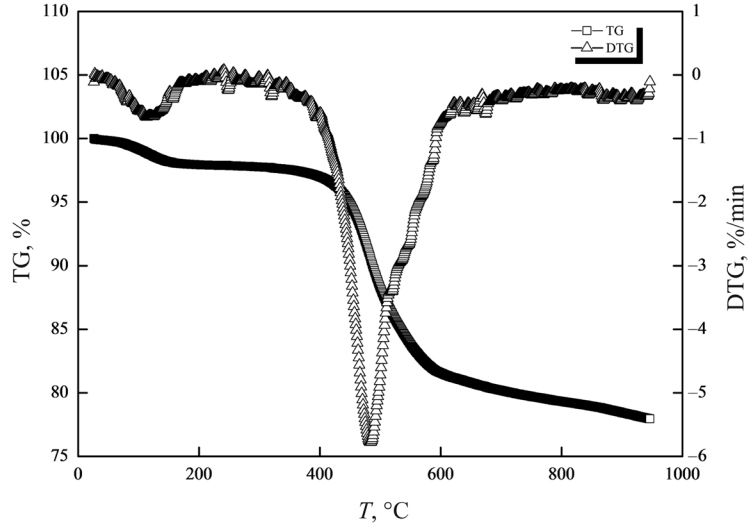

Fig. 1. Pyrolysis TG and DTG curves of oil shale of Fushun west open-cast mine.

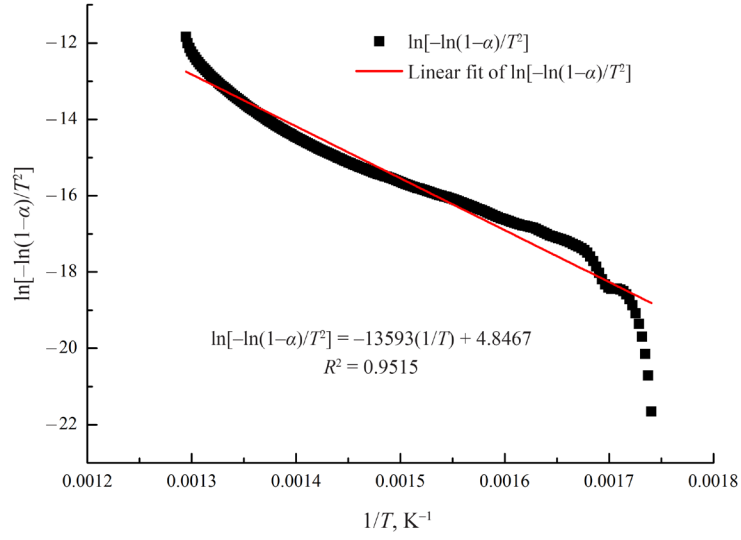

Fig. 2. Linear fitting result of $\ln[-\ln(1-\alpha)/T^2]$ and $1/T$.

As seen from this figure, the activation energy D = 113012.202 J/mol ≈ 113.01 kJ/mol and the frequency factor A = 51919635.76 min^{-1}. Then the pyrolysis rate equations for oil shale at 300 °C, 400 °C and 500 °C can be respectively expressed as follows:

$$\alpha = 1 - e^{-kt} = 1 - e^{-2.64 \times 10^{-3} \cdot t}, \quad (14)$$

$$\alpha = 1 - e^{-kt} = 1 - e^{-0.089 \cdot t}, \quad (15)$$

$$\alpha = 1 - e^{-kt} = 1 - e^{-1.21 \cdot t}. \quad (16)$$

3.2. Verification of the model of oil shale porosity during pyrolysis

The values of porosity model parameters were taken from previous researches: n_c = 4.56%, p_o = 18.9%, p_c = 1.95 *g/cm*^{3}, p_s = 2.05 *g/cm*^{3}, p_o = 1.104 *g/cm*, p_c = 8.19% [23, 24].

The porosity of oil shale during the 30-minute and 60-minute pyrolysis at 300 °C, 400 °C and 500 °C was calculated and the values obtained were compared with experimental values. The results are given in Table 1.

Table 1. Comparison between the calculated and measured values of porosity

Temperature, °C	Time, min	Calculated values, %	Measured values ,% [3, 22]			Absolute error, %		
			Conventional method	Mercury intrusion method	CT method	Conventional method	Mercury intrusion method	CT method
300	60	8.33	7.39	–	–	0.99	–	–
400	30	28.52	–	20.33	24.14	–	8.19	4.38
	60	30.17	18.80	–	–	11.37	–	–
500	30	30.29	–	29.76	33.71	–	0.53	3.42
	60	30.29	25.50	–	–	4.79	–	–

Table 2 reveals that under various temperature conditions there is a good agreement between the experimental porosity values and those calculated by the model with a small error only. The absolute porosity error at 300 °C is the smallest, being larger at 500 °C, and the largest at 400 °C, which is due to the influence of oil shale particle size on pyrolysis. Although oil shale is in a high-temperature environment, the heat transfer and temperature rise also require a certain amount of time to take place. The higher the temperature, the larger the block diameter and the longer the heat transfer time required. The pyrolysis ratio equation established in this research is based on the weight loss data of

Table 2. Mechanical properties of oil shale samples at different temperatures [22]

Temperature, ºC	Measured value of elastic modulus, MPa	Measured value of compressive strength, MPa
Room temperature	3289.33	76.84
200	2443.33	49.60
300	1748.67	34.28
400	1496.00	29.10
500	1104.67	21.34
600	1899.00	20.21

the ground oil shale sample (particle size ≤ 0.2 mm). The size of the oil shale sample measured by the conventional method (approximately 40–50 mm in length in cube rock) is big, while the size of the oil shale sample (Φ3.8 × 15 mm) measured by the mercury intrusion and CT methods is small. Studies have shown that at 475 °C, oil shale with a block diameter of 40–70 mm requires a heat transfer time of 30–40 min [23]. At a lower temperature, 300 °C, the internal and external temperatures of oil shale specimens can be consistent over a short time. The actual conversion ratio of oil shale does not differ much from the theoretical conversion ratio, so the absolute error of oil shale porosity is small at 300 °C. At a higher temperature, 400 °C, it takes a long time for the internal and external temperatures of the specimens to reach the same temperature, and the conversion ratio of 99% is achieved in 51.63 min. A longer heat transfer time will greatly affect the pyrolysis conversion ratio of oil shale, so the absolute porosity error at 400 °C is relatively large. At 500 °C, it takes only 3.80 min for the conversion rate to reach 99%. Although the heat transfer time is further extended, there is still enough pyrolysis time for the actual conversion ratio of oil shale to reach almost the same level with the theoretical conversion ratio, so the absolute error of oil shale porosity is not large. In addition, a comparison showed the measured porosity values to be smaller than the theoretical ones, which may be explained by that the pyrolysis products would more or less remain in the pores of oil shale.

In summary, the model established in this study based on the pyrolysis reaction kinetics can accurately calculate the porosity of oil shale in the pyrolysis process with a small error, which is especially suitable for small-sized specimens.

3.3. Verification of the oil shale elastic modulus model during pyrolysis

Table 2 shows the changes in the mechanical properties of oil shale after complete pyrolysis from room temperature to 600 °C. It can be seen that after entering the pyrolysis stage, due to the thermal decomposition of kerogen, the

elastic modulus and compressive strength drop significantly until 500 °C. At 600 °C, the elastic modulus increases and the compressive strength decreases, but these changes are small. The changes in the porosity, compressive strength and elastic modulus of oil shale during the pyrolysis process were mainly caused by that of kerogen. Compared with the pyrolysis of kerogen which mainly took place in the temperature range of 300–500 °C, the pyrolysis of oil shale at 500–600 °C also involved that of other substances such as fixed carbon. Therefore, compared with 500 °C, the elastic modulus and compressive strength of oil shale at 600 °C changed but a little [22].

As seen above, the pyrolysis of oil shale starts at 300 °C. To exclude the effect of water in oil shale on the pore pressure provided by kerogen, in this study, the elastic modulus of oil shale at 200 °C is taken as the basic value of the pre-pyrolysis elastic modulus to calculate the elastic moduli at 300 °C, 400 °C and 500 °C during pyrolysis.

3.3.1. Calculation of pore pressure during pyrolysis

The compressive strength of oil shale is composed of the compressive strength of the oil shale skeleton and the pore pressure provided by kerogen, which can be expressed as Equation (17):

$$\sigma = \sigma' + u. \tag{17}$$

The compressive strength of oil shale, i.e. of the oil shale skeleton, after complete pyrolysis at 300 °C, 400 °C and 500 °C was statistically analyzed, and the mechanical damage of the skeleton was found to linearly increase with temperature (Fig. 3).

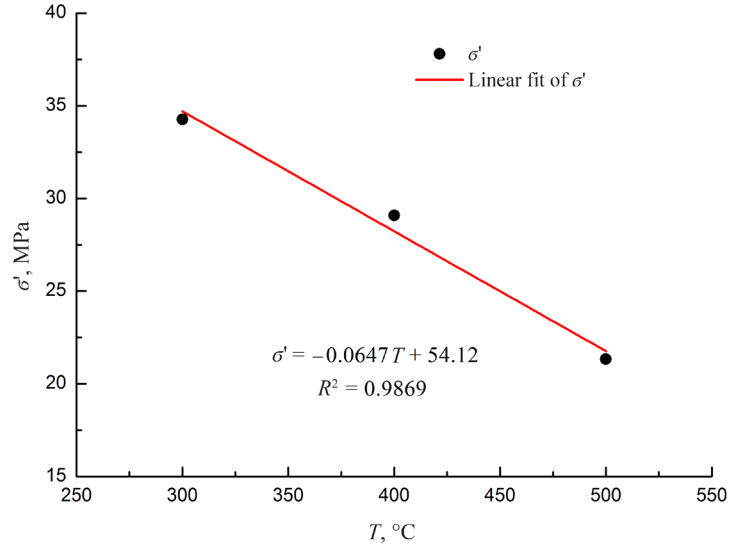

Fig. 3. Linear fitting result of the oil shale skeleton compressive strength and temperature.

As seen from Figure 3, the linear fitting equation of the compressive strength of the oil shale skeleton with temperature is expressed as Equation (18):

$$\sigma' = -0.0647T + 54.12,\ R^2 = 0.9869. \tag{18}$$

The calculated compressive strength value of the oil shale skeleton at 200 °C is 41.18 MPa. At 200 °C, the water in oil shale is completely evaporated and the pyrolysis of the oil parent material has not yet occurred. So, the pore pressure provided by the oil parent material in oil shale can be calculated as follows:

$$u = \sigma_{200\,^{\circ}\mathrm{C}} - \sigma'_{200\,^{\circ}\mathrm{C}} = 49.6 - 41.18 = 8.42 \text{ MPa}. \tag{19}$$

3.3.2. Verification of the elastic modulus of oil shale during pyrolysis

The elastic modulus of oil shale at different pyrolysis temperatures was continuously simulated and calculated. The results are shown in Figure 4.

The elastic modulus of oil shale during pyrolysis is difficult to measure in real time. To avoid the error effect caused by the heat transfer time, the calculated elastic modulus values of oil shale after full pyrolysis at 300 °C, 400 °C and 500 °C (calculated at a conversion ratio of 0.99) are compared with the experimental data obtained under the corresponding conditions for verification, as shown in Table 3.

Table 3 reveals the closeness of the calculated and experimental values of the oil shale elastic modulus, while the relative error is small. These results also confirm the correctness of the hypothesis made and the calculated model established in this study.

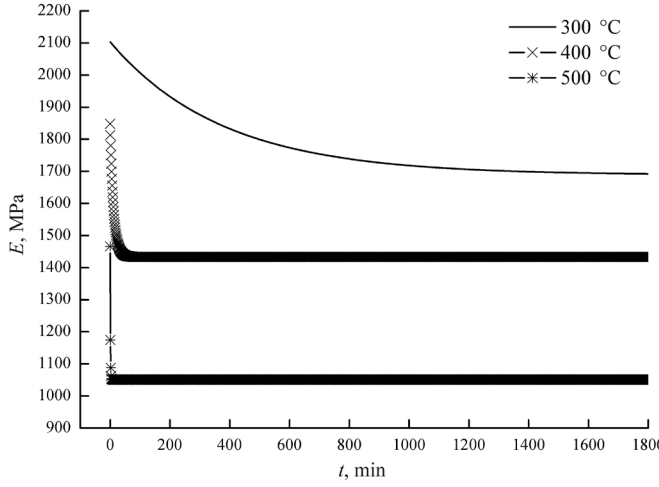

Fig. 4. The elastic modulus of oil shale during pyrolysis.

Table 3. Comparison between the calculated and measured values of elastic modulus

Temperature, ºC	Measured value of elastic modulus. MPa	Calculated value of elastic modulus, MPa	Relative error, %
300	1748.67	1688.66	3.43
400	1496.00	1433.49	4.18
500	1104.67	1051.22	4.84

3.4. Establishment of the oil shale permeability model during in situ pyrolysis

3.4.1. Quantitative relationship between oil shale porosity and permeability

In fitting data of a previous research [22], in this study, the quantitative relationship between the porosity and permeability of Fushun oil shale was established, as shown in Figure 5 and by Equation (20):

$$k = 0.4301 \cdot n^{1.3988},\ R^2 = 0.9338, \tag{20}$$

where k is the permeability of oil shale and n is the porosity of oil shale.

A previous study [25] found that rock porosity was positively correlated with permeability as a power function. Equation (20) presented in the current study is consistent with this finding.

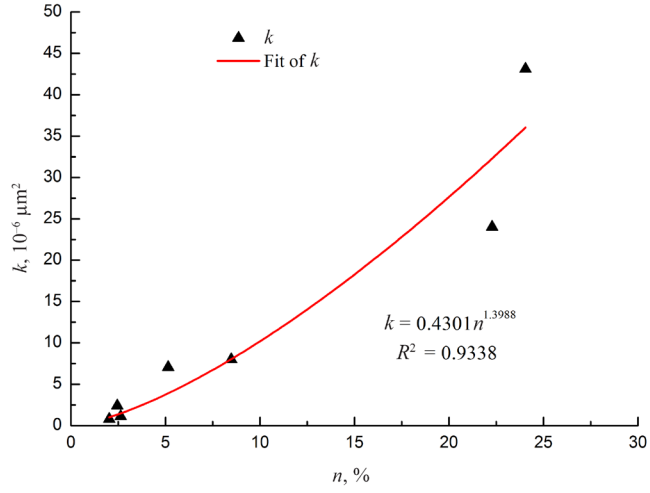

Fig. 5. Fitting result of the porosity and permeability of oil shale.

3.4.2. Model of permeability and calculated oil shale permeability during in situ pyrolysis

By substituting Equation (12) into Equation (20), the model of Fushun oil shale permeability during in situ pyrolysis can be expressed as Equation (21):

$$k_t = 0.4301 \cdot \left(\frac{n' - \varepsilon_k}{1 - \varepsilon_k} \right)^{1.3988}, \tag{21}$$

where k_t is the permeability of oil shale during pyrolysis under in situ pressure.

Based on Equation (21), the permeability of oil shale during the pyrolysis process at 300 °C, 400 °C and 500 °C at vertical pressures of 1 MPa, 5 MPa and 10 MPa, respectively, was calculated, the results are shown in Figure 6.

Figure 6 displays both temperature and pressure to influence the permeability of oil shale during pyrolysis. In case of the same temperature and time of pyrolysis, permeability decreases with increasing pressure. However, the permeability of oil shale is mainly affected by temperature and increases rapidly with it. At 300 °C, the oil shale permeability increases slowly. At temperatures of 400 °C and 500 °C, it increases rapidly, decreasing thereafter. After a 6-minute pyrolysis, the permeability increase ratio at 500 °C is the highest, 1330.79–1515.96%, being at 400 °C rather similar, approximately 1319.72–1465.62%, and at 300 °C the lowest, 133.80–144.72%. Although the permeability of oil shale increases significantly at 500 °C, its absolute permeability is still low, the maximum being only 50.65×10^{-6} μm^2, which is considered poor. According to the permeability classification [24], the pyrolyzed oil shale layer belongs to the ultra-low permeability rock layer, which means that the hydrogeological environment of the mining area after in situ pyrolysis is relatively safe.

3.5. Discussion

This study does not consider the process of heat conduction during pyrolysis, and by default, the temperature is always the same. The heat transfer time of small-sized specimens is shorter, so the permeability model during in situ pyrolysis is more easily applicable to small oil shale samples. To accurately simulate the permeability change during the in situ pyrolysis of large block oil shale, it is necessary to combine the heat transfer equation with the established permeability model during in situ pyrolysis. Previous studies have shown that the time required for the temperature of block oil shale to reach consistency is in direct proportion to the square of the block diameter [25, 26], providing a theoretical basis for a further modification of this model in the future.

The effect of thermal cracking on permeability is not considered in this study, mainly because this phenomenon is the result of an uneven thermal expansion of the rock, which is mostly controlled by the rock heterogeneity

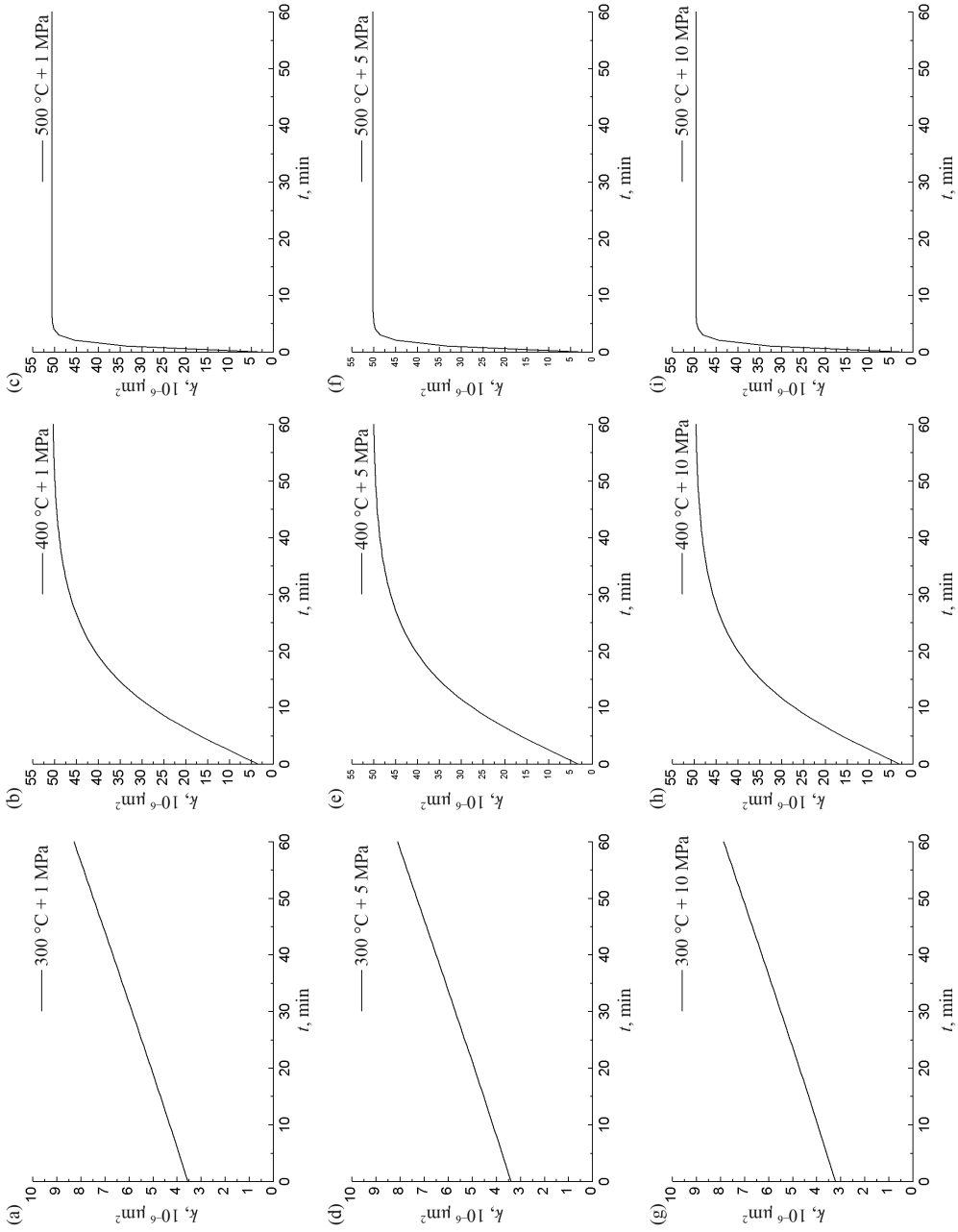

Fig. 6. Simulation results of oil shale permeability during in situ pyrolysis.

and reveals certain randomness. Meanwhile, the currently available theoretical model for thermal cracking is far from being perfect [27–29]. An in-depth study of the formation mechanism of thermal cracking and its impact on permeability, as well as a further improvement of the permeability model of oil shale during in situ pyrolysis will be the directions of future research.

4. Conclusions

1. Models for oil shale porosity and elastic modulus during pyrolysis are established. The theoretical calculated values are basically consistent with the measured values, with a small error only. Based on the above two models, combined with the fitting relationship between porosity and permeability, the permeability model during in situ pyrolysis is established.
2. The simulation results show that under in situ pyrolysis conditions, the permeability of oil shale is mainly affected by temperature and increases with increasing temperature. The higher the temperature, the higher the rate of increase in permeability. After in situ pyrolysis, the absolute permeability of oil shale is still low and has a little impact on the hydrogeological environment of the mining area.
3. The model of oil shale permeability during in situ pyrolysis is easily applicable to small oil shale samples. For large block oil shale, the heat conduction process will become a key controlling factor affecting its overall permeability. Combining the heat transfer equation with the established permeability model during in situ pyrolysis, constructing a permeability model which is suitable for full-sized oil shale is the direction of future research.

Acknowledgments

This work was supported by the National Natural Science Foundation of China (Grant No. 51604182), the Natural Science Foundation of Shanxi Province, China (Grant Nos. 201801D221329, 201701D121129), the Natural Science Foundation of Hebei Province, China (Grant Nos. E2019402361, E2020402075), the Postdoctoral Research Projects of Hebei Province, China (Grant No. B2020003010), the Science and Technology Research Project of Hebei Higher Education (ZD2021309) and the Innovation Fund Project of Hebei University of Engineering (Grant No. BSJJ1930). Associate Professor Kang Zhiqin is gratefully acknowledged for providing oil shale thermogravimetric analysis data.

REFERENCES

1. Le Doan, T. V., Bostrom, N. W., Burnham, A. K., Kleinberg, R. L., Pomerantz, A. E., Allix, P. Green River oil shale pyrolysis: semi-open conditions. *Energy Fuels*, 2013, **27**(11), 6447–6459.
2. Huan, Z., Weiping, S., Dali, D., Zhang, C. Numerical simulation of in situ combustion of oil shale. *Geofluids*, 2017, **2017**, 1–9.
3. Kang, Z. *The Pyrolysis Characteristics and In-Situ Hot Drive Simulation Research that Exploit Oil–Gas of Oil Shale*. PhD thesis, Taiyuan University of Technology, 2008 (in Chinese with English abstract).
4. Kang, Z., Yang, D., Zhao, Y., Hu, Y. Thermal cracking and corresponding permeability of Fushun oil shale. *Oil Shale*, 2011, **28**(2), 273–283.
5. Eseme, E., Krooss, B. M., Littke, R. Evolution of petrophysical properties of oil shales during high-temperature compaction tests: Implications for petroleum expulsion. *Mar. Petrol. Geol*., 2012, **31**(1), 110–124.
6. Tiwari, P., Deo, M., Lin, C. L., Miller, J. D. Characterization of oil shale pore structure before and after pyrolysis by using X-ray micro CT. *Fuel*, 2013, **107**, 547–554.
7. Zhao, J., Feng, Z., Yang, D., Kang, Z. Study on pyrolysis and internal structure variation of oil shale based on 3D CT images. *Chin. J. Rock Mech. Eng.*, 2014, **33**(1), 112–117 (in Chinese with English abstract).
8. Jiang, X., Chu, T. M., Liang, X. J., Xiao, C. L., Yan, B. Z., Wang, Y. N. Impact of mining oil shale in different methods on the environment. In: *Environment, Energy and Sustainable Development* (Sung, W., Kao, J., Chen, R., eds.). Taylor & Francis Group, London, 2014, 359–363.
9. Qiu, S. *Experimental Study on the Impacts of Oil Shale In-situ Pyrolysis on Groundwater Hydrochemical Characteristics*. PhD thesis, Jilin University, 2016 (in Chinese with English abstract).
10. Bai, F., Sun, Y., Liu, Y., Guo, M. Evaluation of the porous structure of Huadian oil shale during pyrolysis using multiple approaches. *Fuel*, 2017, **187**, 1–8.
11. Burnham, A. K. Porosity and permeability of Green River oil shale and their changes during retorting. *Fuel*, 2017, **203**, 208–213.
12. Geng, Y., Liang, W., Liu, J., Cao, M., Kang, Z. Evolution of pore and fracture structure of oil shale under high temperature and high pressure. *Energy Fuels*, 2017, **31**(10), 10404–10413.
13. Geng, Y., Liang, W., Liu. J., Kang, Z., Wu, P., Jiang, Y. Experimental study on the variation of pore and fracture structure of oil shale under different temperatures and pressures. *Chin. J. Rock Mech. Eng.*, 2018, **37**(11), 2510–2519 (in Chinese with English abstract).
14. Geng, Y., Liu, J., Bi, J. Experimental study of pore structure of Fushun oil shale after pyrolysis. *Coal. Technol.*, 2018, **37**(6), 84–86 (in Chinese with English abstract).
15. Geng, Y., Liang, W., Liu. J., Wu, P., Zhao, J. Experimental study on the law with permeability of Fushun oil shale under high temperature and triaxial stresses.

J. Taiyuan. Univ. Technol., 2019, **50**(3), 272–278 (in Chinese with English abstract).
16. Guo, S., Geng, L. Study on pyrolysis kinetics of oil shales by thermogravimetry. *J. Fuel Chem. Technol.*, 1986, **14**(3), 211–217 (in Chinese with English abstract).
17. Cai, M. *Rock Mechanics and Engineering*. Science Press, Beijing, 2002 (in Chinese).
18. Coats, A. W., Redfern, J. P. Kinetic parameters from thermogravimetric data. *Nature*, 1964, **201**(4914), 68–69.
19. Weitkamp, A. W., Gutberlet, L. C. Application of a micro retort to problems in shale pyrolysis. *Ind. Eng. Chem. Proc. Des. Dev.*, 1970, **9**(3), 386–395.
20. Shih, S.-M., Sohn, H. Y. Nonisothermal determination of the intrinsic kinetics of oil generation from oil shale. *Ind. Eng. Chem. Proc. Des. Dev.*, 1980, **19**(3), 420–426.
21. Braun, R. L., Rothman, A. J. Oil-shale pyrolysis: Kinetics and mechanism of oil production. *Fuel*, 1975, **54**(2), 129–131.
22. Zhao, J. *Experimental Study on the Microscopic Characteristics and Mechanical Property of Oil Shale under High Temperature & Three-Dimensional Stress*. PhD thesis, Taiyuan University of Technology, 2014 (in Chinese with English abstract).
23. Qian, J., Yin, L. *Oil Shale: Petroleum Alternative*. China Petrochemical Press, Beijing, 2008 (in Chinese).
24. Yang, S., Wei, J. *Reservoir Physics*. China Petrochemical Press, Beijing, 2004 (in Chinese).
25. Qin, K. Investigation on the constitution and structure of Maoming and Fushun oil shale. Average building block of organic matter. *J. Fuel Chem. Technol*., 1986. **14**(1), 3–10 (in Chinese with English abstract).
26. Liu, G. *Petroleum Geology*. China Petrochemical Press, Beijing, 2009 (in Chinese).
27. Yu, Q., Zheng, C., Yang, T., Tang, S., Wang, P., Tang, C. Meso-structure characterization based on coupled thermal-mechanical model for rock failure process and applications. *Chin. J. Rock Mech. Eng.*, 2012, **31**(1), 42–51 (in Chinese with English abstract).
28. Feng, Z., Zhao, Y. Pyrolytic cracking in coal: Meso-characteristics of pore and fissure evolution observed by micro-CT. *J. China Coal Soc.*, 2015, **40**(1), 103–108 (in Chinese with English abstract).
29. Yan, C. Simulating thermal cracking of rock using FDEM-TM method. *Chin. J. Rock Mech. Eng.*, 2018, **40**(7), 1198–1204 (in Chinese with English abstract).